

High temperature, steam oxidation performance of advanced, highly alloyed steels and Ni based alloys as candidates for the structural materials in Ultra Super Critical (USC) Coal Power Plants

Tomasz DUDZIAK¹, Vinay DEODESHMUKH², Lukasz BORON¹, Jerzy SOBCZAK¹, Natalia SOBCZAK¹, Laurel BACKRET³

¹*Foundry Research Institute Zakopianska 73, 30-418
Krakow/Poland*

tomasz.dudziak@iod.krakow.pl, lukasz.boron@iod.krakow.pl, jerzy.sobczak@iod.krakow.pl,
natalia.sobczak@iod.krakow.pl,

²*Haynes International, 1020 West Park Avenue, Kokomo, United States of America,*

VDeodeshmukh@haynesintl.com

³*Sandmeyer Steel Company, One Sandmeyer Lane,
Philadelphia, PA 19116*

l.a.backert@sandmeyer.com

Abstract

Reduction in CO₂ emissions from coal-fired power plants is one of the major challenges in order to decrease global warming effect. In energy sector, the aim to reduce CO₂ emission can be achieved by increasing the operating temperature (and pressure) of water steam system, which results in an increase in overall coal fired power plant efficiency. Currently the main components of coal fired power plants are made from the materials designed years ago; to meet harsh eco criteria such materials are not suitable for harsh conditions of modern coal-fired power plant. Subcritical power stations are main contributor in CO₂ emission globally, with high CO₂ emission and low efficiency ~ 37 %. The next-gen coal-fired power plants have potential to reach 55% efficiency, taking into account, that 1% increase in absolute efficiency results in as much as 3% reduction in CO₂ emissions, 55 % of CO₂ lower emission achieved. Modern, advanced coal fired power stations operating under Ultra Super Critical (USC) or Advanced Ultra Super Critical (AUSC) conditions experience temperatures exceeding 750 °C. Super heated steam at high temperatures causes accelerated degradation of low-alloyed steels or even medium Cr steels. Therefore for aggressive, steam oxidation conditions highly alloyed steels and advanced Ni based alloys. These materials must provide excellent steam oxidation resistance at high temperature via the formation of chromia scale. In this study, the steam oxidation behaviour of highly alloyed steels 309S, 310S, HR3C and advanced Ni based alloys: Haynes[®] 230[®], alloy 263, alloy 617, Haynes[®] 282[®] has been examined. The materials have been exposed for 2000 hours at 800 °C in unique close loop water – steam system.

Keywords: Ni based alloy, steam oxidation, phase development

Introduction

Raising environmental awareness is driving the global economy towards the reduction of CO₂ emissions and fuel consumption. The power energy sector is contributing to these goals by increasing power generation efficiency; it can be achieved by increasing temperature and pressure of steam entering the steam turbine and efficiency of electric output [1,2,3]. Higher operational temperatures can affect performance of boiler components especially when low alloyed steels are used. Steam oxidation of high temperature resistant alloys has an important impact on the power plant lifetime and efficiency. Higher operational temperatures significantly accelerate oxidation processes, leading to the development of thick, non-protective Fe-rich oxides with flaky, brittle structures susceptible to scale spallation. Additionally, fast oxide growth and high metal loss significantly reduces heat transfer ability in order to withstand high steam pressures [4,5]. The changes in coal fired power plants, in respect to temperature and pressure can be briefly characterised as follows [6]:

- 1) 70s of XX century: 538 °C/538°C/16.7 MPa,
- 2) 80s of XX century: 540 °C/560°C/25.0 MPa,
- 3) 90s of XX century: 560 °C/580°C/27.0 MPa,
- 4) Turn of the century XX → XXI: 600 °C/620 °C/29,0 MPa USC,
- 5) In 2020 of XXI century: 700 °C/720 °C/350 MPa AUSC.
- 6)

As seen *ultra-super critical* (USC) and AUSC *advanced ultra super critical technology* present the harshest conditions, where the steels developed over 50 – 60 years ago cannot be used according to the following list [7]:

- 1) Ferritic steels: $p < 26$ MPa, 545 °C,
- 2) Ferritic Martensitic steels: $p = 26$ MPa, 545 °C,
- 3) Austenitic steels: 29 MPa, 600 °C,
- 4) Ni based alloys: $p > 35$ MPa, $T > 700$ °C.

Even today, steels such as: T22 (10CrMo910), T91 (X10CrMoVNb9-10), E1250 (X10CrNiMoMnNbVB15-10-1), 316L (X2CrNiMo18-14-3) and TP347HFG (18Cr9Ni3CuNbN) are broadly used in energy sector; however, those materials do not always meet criteria in harsh conditions due to lack of the formation of long standing thin and stable Cr₂O₃ scale. Nevertheless, the steels containing up to 18 wt % Cr in the matrix possess the ability to form Cr₂O₃ scale but often under long term exposures are susceptible to catastrophic corrosion degradation. This occurs due to chromia evaporation and such mechanism can be observed in 304L type austenitic stainless steel [8]. Currently, particular attention is paid for the materials with higher content of Cr than 20 wt%. The alloys under consideration, two solid-solution strengthened alloys; Haynes[®] 230[®], 617 alloy and two (γ') gamma - prime strengthened alloys - 263 and Haynes[®] 282[®] and high alloyed steels rich in Cr - 309S, 310S and HR3C have been tested under 1 bar pressure in 100% water – steam – water system at 800 °C for 2000 hours. In this work, kinetic weight change measurements have been performed by traditional discontinuous method using digital balance with high accuracy. Post investigations of the exposed samples have been performed using Scanning Electron Microscopy (SEM) in Backscatter Electron mode (BSE). Phase development and changes upon steam oxidation have been examined every 1000 hours using Bragg Brentano technique and grazing incident $\alpha=1^\circ$ and $\alpha=3^\circ$ to study the oxide scales development. Finally, internal oxidation process on cross-sectioned samples have been conducted

Experimental Procedure

Materials

In the study, in total seven materials have been exposed; two solid-solution strengthened alloys; alloy 617 and Haynes[®] 230[®], two (γ') gamma - prime strengthened materials; alloy 263 and Haynes[®] 282[®] as well as high alloyed steels rich in Cr: 309S, 310S and HR3C. Prior to steam oxidation test chemical compositions of delivered materials has been investigated using EDS analyser. **Table 1** and **Table 2** show nominal compositions according to producer certificates of the Ni based alloys and high-alloyed steels respectively.

Table 1 Chemical composition of Ni based alloys (wt%) used in steam oxidation work

	Ni	Fe	Cr	Co	Mo	Si	Mn	Cu	La	Ti	Al	C	W	B
alloy 263	Bal.	0.6	20	20	6	0.4	0.6	0.2	-	1.2	0.6	0.06	-	-
alloy 617	Bal.	1	22	12.5	9	-	-	-	-	0.3	1.2	0.07	-	-
Haynes [®] 230 [®]	57	3	22	5	2	0.4	0.5		0.02		0.3	0.1	14	0.015
Haynes [®] 282 [®]	Bal.	1.5	20	10	8.5	0.15	0.3	-	-	2.1	1.5	0.06	-	0.05

Table 2 Chemical composition of high alloyed steels (wt%) used in steam oxidation work

	Fe	Cr	Mn	Ni	P	S	Si	C	Nb	N
310S	Bal.	25	2	21	0.045	0.03	1.5	0.08		
309S	Bal.	23	2	14	0.045	0.03	0.75	0.2		
HR3C	Bal.	25	1.2	20	0.04	0.03	0.4	0.06	0.45	0.2

Prior to the steam oxidation test at 800 °C the alloy samples were cut out from the plate in size of small squares with dimensions 10 x 10 x 1.5 mm. As mentioned, HR3C alloy was delivered as a tube section, the material was machined into tube segment, which had dimensions of ~ 15 mm long, x 10 mm wide, chord with a 4 mm wall thickness. The surface of the steels and Ni alloys was ground to 600 grid surface finish. Furthermore, the samples were cleaned in acetone at 40 °C for 20 min using an ultrasonic bath. The samples before and during exposure were accurately weighed using digital balance with a resolution of $m \pm 0.01$ mg for masses $m = < 80$ g. The balance was calibrated frequently using its internal calibration function and periodically with test weights.

Steam oxidation experiment

High temperature experimental rig, with ability to produce pure water steam conditions is presented in **Figure 1**.

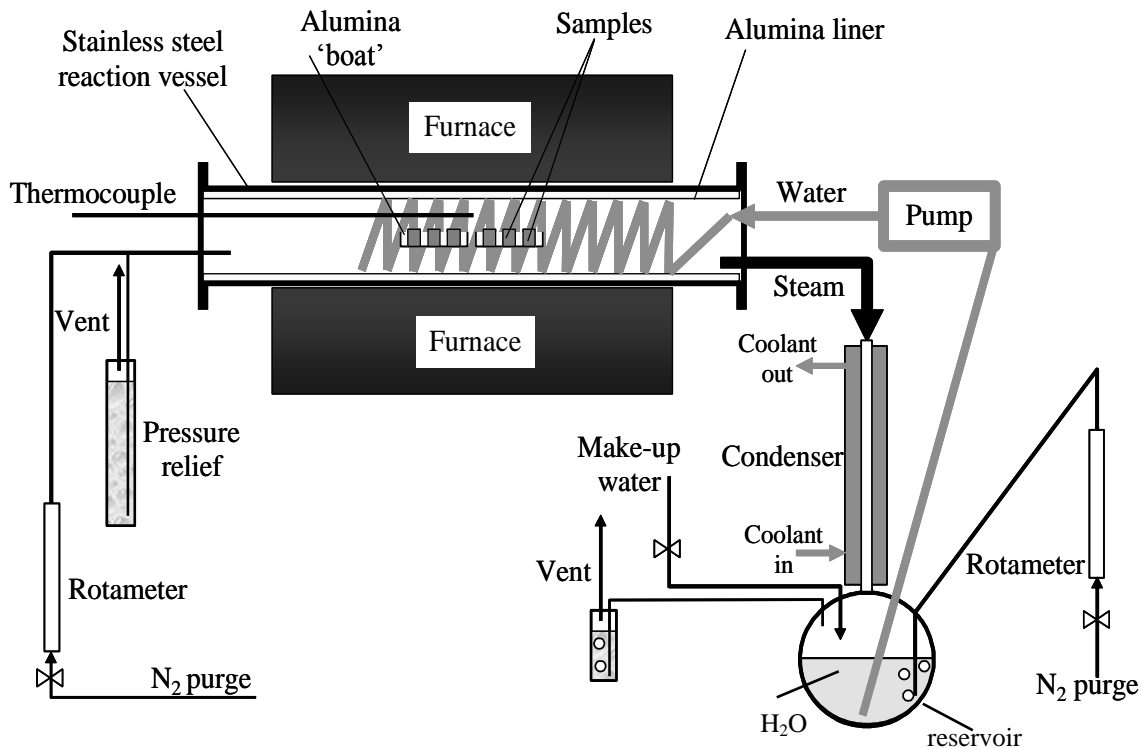


Figure 1 Steam oxidation rig used in this study

In this type of steam oxidation test set-up [9]; 100% pure steam was generated by pumping water from a reservoir placed underneath the furnace. In the furnace water steam passed over the tested samples and flown into a condenser before the water returned to the reservoir. The water used in the reservoir was double de-ionised. The whole system was sealed using stainless steel flanges from both ends, prior to the test the whole system was purged for 2 hours using oxygen free nitrogen (OFN). This purge continues through the water reservoir throughout the samples exposure period to minimize the level of oxygen in the system in order to reduce partial pressure of oxygen dissolved from the ambient atmosphere. Prior to the exposure, the furnace calibration was required in order to detect the hot zone. The calibration process ensured placement of the samples in the furnace at test temperature with accuracy ± 5 °C.

XRD investigations

The XRD investigations have been conducted by means of D500 Kristalloflex with monochromatic X-ray sources Cu ($\lambda K\alpha = 1.54\text{\AA}$) and EMPYREAN Panalytical with X-ray source Cu using Ni filter after 1000 and 2000 hours. The phase analyses have been performed using two techniques; Bragg-Bentano (BB) geometry and the geometry of constant angle called grazing incidence using $\alpha = 1^\circ$ and $\alpha = 3^\circ$. In Bragg-Bentano (BB) geometry, depth penetration of X-rays can be estimated using the following formula:

$$X = \frac{-\ln(1-Gx)\sin\theta}{2\mu} \quad (1)$$

Where:

- Gx donates the intensity of the primary X-ray, giving important information related to irradiation volume.
- μ linear absorption coefficient

In the grazing angle method, X-rays depth penetration was calculated via the following formula:

$$X = \frac{-\ln(1-Gx)}{\left\{ \mu \left[\frac{1}{\sin\alpha} + \frac{1}{\sin(2\theta-\alpha)} \right] \right\}} \quad (2)$$

Where:

- Gx donates the intensity of the primary X-ray, giving important information related to irradiated volume, this value is equivalent to 0.95 (95%)
- μ - linear absorption coefficient
- α - incidence angle

The calculated values of Gx where assumption of Gx = 95% are shown in **Table 3**.

Table 3 Depth penetration for the selected samples and the selected phases using two different geometries

Sample/phase	BB geometry	grazing incidence $\alpha=1^\circ$	grazing incidence $\alpha=3^\circ$
alloy 617	4.33 - 10.96 μm	0.43 μm	1.26 μm
alloy 263	3.91 - 9.91 μm	0.39 μm	1.14 μm
Haynes [®] 230 [®]	4.23 - 10.71 μm	0.42 μm	1.23 μm
Haynes [®] 282 [®]	4.64 - 11.76 μm	0.47 μm	1.35 μm
310S	2.89 - 7.32 μm	0.29 μm	0.84 μm
309S	2.58 - 6.53 μm	0.26 μm	0.75 μm
HR3C	2.76 - 6.99 μm	0.28 μm	0.8 μm

Results and discussion

Kinetics

Steam oxidation kinetic test results at 800 °C for 2000 hours for Ni based alloys and the highly alloyed Fe based materials with Cr content higher than 20 wt% are shown in **Figure 2A** and **2B** respectively.

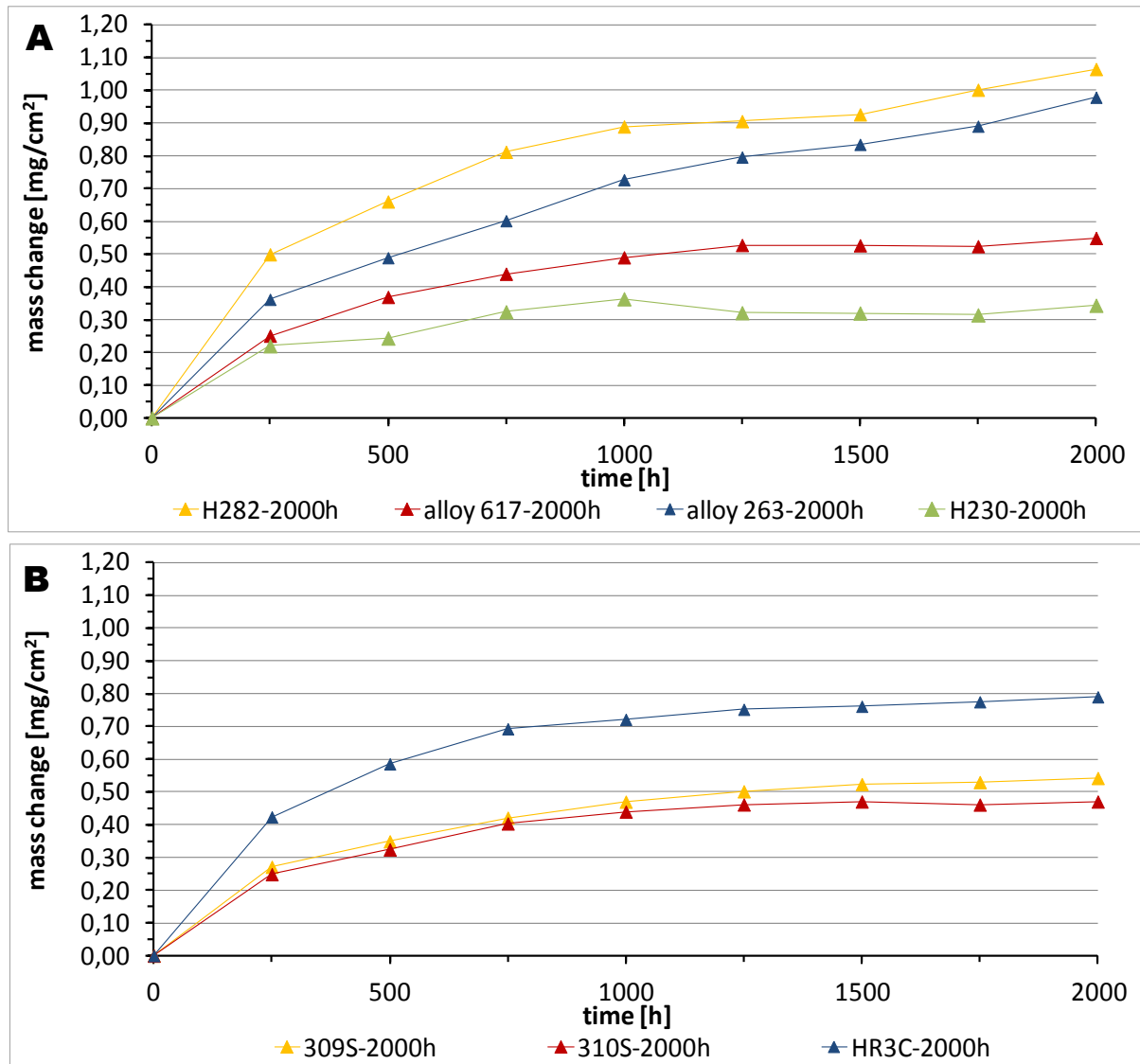


Figure 2 Mass change data of Ni based alloys (A) and highly alloyed steels (B) exposed at 800 °C for 2000 hours

The 230 alloy showed the lowest weight gain, while 310S and 309S indicated lower weight gain the other alloys. The highest weigh gain has been observed in HR3C material among the exposed stainless steels. Haynes[®] 282[®] showed the highest weight gain among the alloys tested. The most promising material, with the lowest mass gain after 2000 hours at 800 °C was Haynes[®] 230[®], the alloy showed reduced mass change of about 0.9 mg/cm², than that offered by Haynes[®] 282[®]. The Haynes[®] 282[®] material is (γ') gamma - prime strengthened materials similar to alloy 263, however Haynes[®] 230[®], and alloy 617 are two solid-solution strengthened alloys, the results indicate that precipitation of Ni₃(Al,Ti) phase under steam oxidation conditions at high temperature showed negative effect in terms of mass gain of the

material. In comparison to Ni based alloys, two steels (309S, 310S) contain Si in the metal matrix while in comparison HR3C steel with reduced Si content, exhibited the highest weight gain. The alloys 309S, and 310S indicated almost the same mass gain after 2000 hours, however, the alloy HR3C showed higher mass. The observed findings suggest, that despite of high Cr content in HR3C (25 wt%) the steel showed the formation of oxide scale with decreased resistance in comparison to 309S and 310S steel. Furthermore, based on chemical composition of the exposed steels, it can be noted that higher Si content in 310S than in 309S positively influence the corrosion resistance. The weight gain kinetics clearly showed that none of the alloys underwent scale spallation or scale vaporisation. The Cr_2O_3 vaporisation requires the presence of O_2 in the environment which is virtually absent in steam, hence all alloys were resistant to scale evaporation.

Surface microstructures

Figure 3 shows surface microstructures of the Ni based alloys exposed to steam oxidation at 800 °C for 2000 hours.

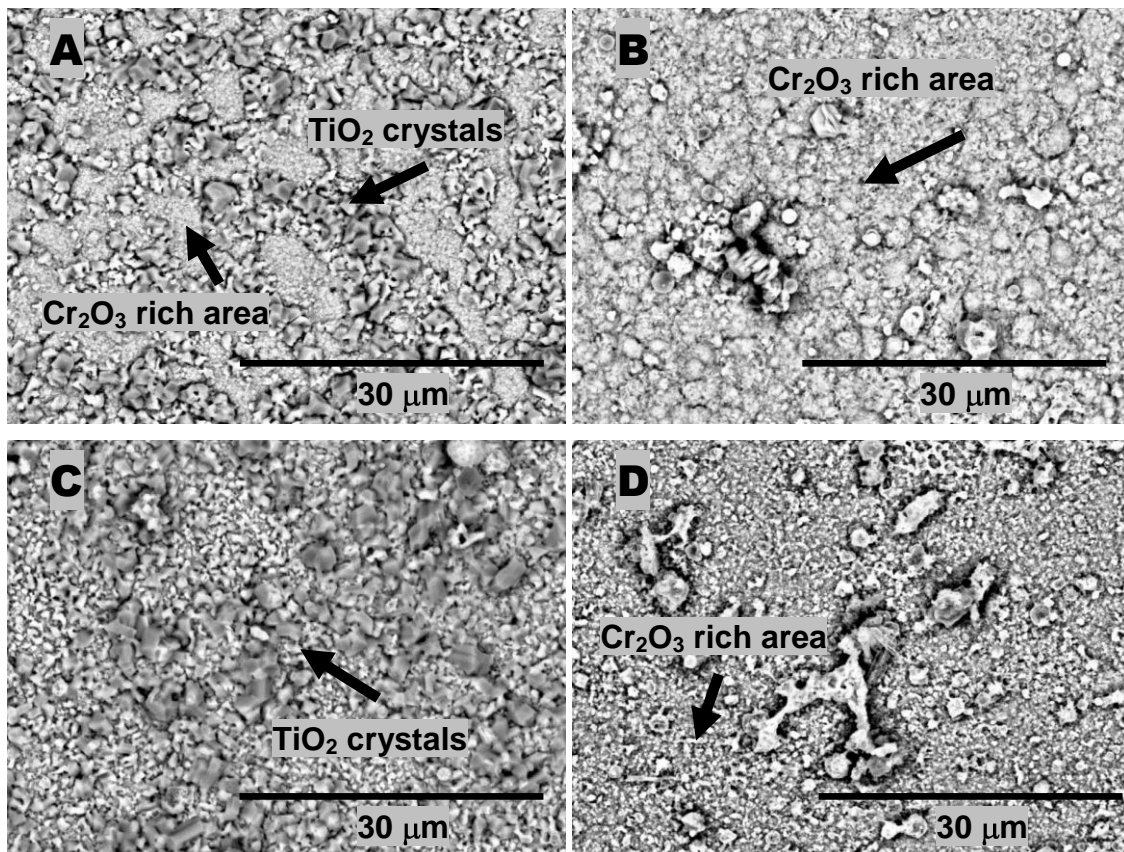


Figure 3 Surface microstructures developed at 800 °C for 2000 hours in steam atmosphere for: A) Haynes[®] 282[®], B) alloy 617, C) alloy 263, and D) Haynes[®] 230[®]

The exposed alloys showed different microstructures developed under steam oxidation conditions, the microstructure varieties are influenced by processing of Ni based alloys. Two solid-solution strengthened alloys; alloy 617, Haynes[®] 230[®] developed the oxide scale richer in Cr than two (γ') gamma - prime strengthened alloys; alloy 263 and Haynes[®] 282[®] where oxidation of Ti from (γ') gamma – prime $\text{Ni}_3(\text{Al,Ti})$ phase occurred at 800 °C. The observed

results, are in good correlation with kinetic data, where two (γ') gamma - prime strengthened alloys as well indicated higher mass change than that observed for two solid-solution strengthened alloys. Furthermore, it appears that after 2000 hours of oxidation Haynes[®] 230[®] offer improved oxidation resistance than that offered by Haynes[®] 282[®] alloy. The Haynes[®] 230[®] had sufficient concentration of Cr in the metal matrix to support development of a protective scale. Whereas, Haynes[®] 282[®] Cr reservoir depleted to the critical level, under which TiO₂ crystals started to develop at 800 °C resulting the formation of semi protective scale with tendency to reach higher values of mass change.

Figure 4 shows surfaces of the exposed steels in pure steam atmosphere under 1 bar pressure at 800 °C for 2000 hours.

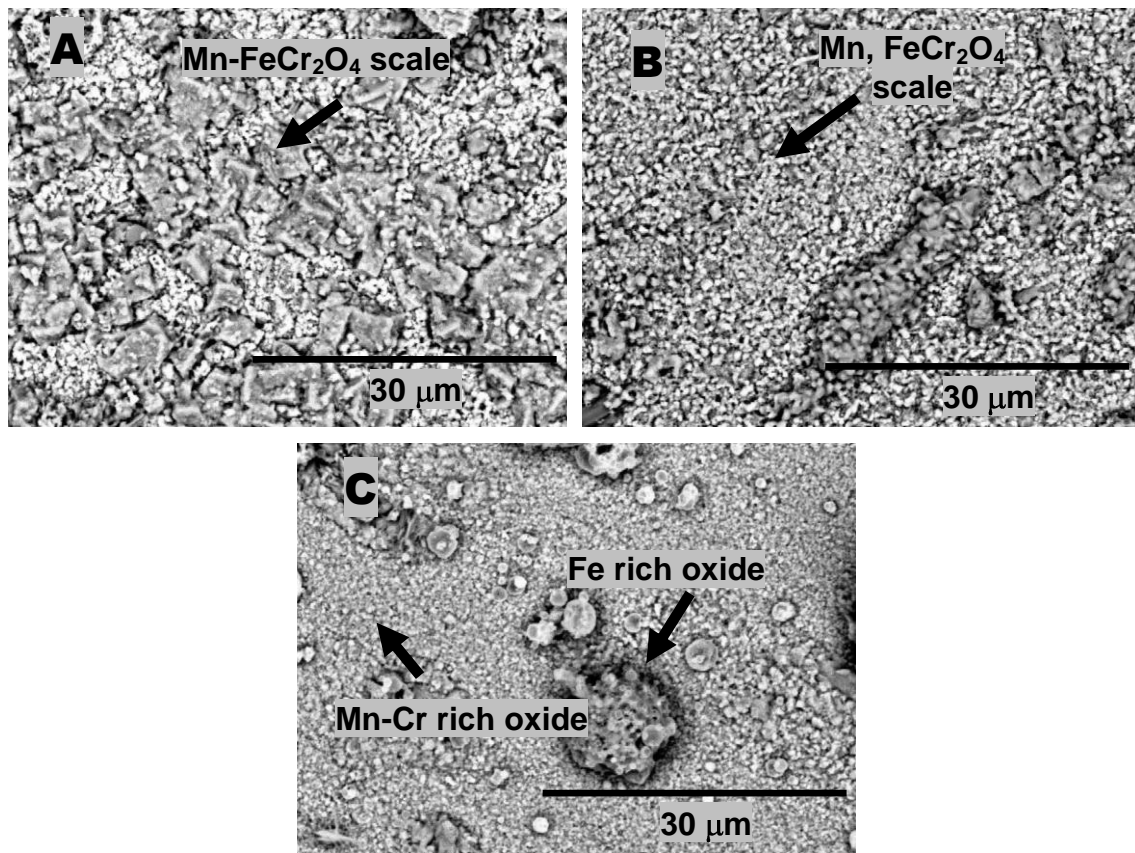


Figure 4 Surface microstructures developed at 800 °C for 2000 hours in steam atmosphere for: A) 309S, B) 310S and C) HR3C steel

The surface microstructure developed under steam oxidation conditions varies from the steel to steel, however two Mn-Si steels 309S and 310S showed development of similar microstructures where rich Mn rich – Fe-Cr₂O₄ oxide developed, the crystals developed on the surface reached around 3 – 4 µm thick and have been distributed evenly on the exposed surface. The surface of 310S steel compared to 309S steel developed similar crystals in terms of chemical composition, however the present crystals were much smaller. Occasionally, the surface microstructure under steam oxidation conditions has been enriched in Si indicating the formation of Si containing phases. Under steam atmosphere, the steel with 25 wt% Cr developed similarly to 309S and 310S steels adherent, steam oxidation resistant oxide scale.

The crystal structures developed in HR3C steel showed different microstructure than that observed 309S and 310S steels. Here, the surface microstructure developed in steam conditions at 800 °C formed thinner crystals consisting mainly Fe-Cr and addition of Mn suggesting development of Mn-Fe-Cr₂O₄ spinel phase. In contrast to 309S and 310S steels, rich HR3C materials developed Fe₃O₄ phase nodules on the exposed surface. The nodules have been observed randomly on the surface, the measured size of the nodules reached 15 μm.

XRD studies

The XRD analyses have been performed after 1000 hours and 2000 hours respectively in order to observe phase changes under steam oxidation conditions at 800 °C. **Figure 5** and **6** show XRD patterns for Ni based alloys and Fe based materials respectively. The investigations have been conducted after 1000 and 2000 hours for better phase development observation.

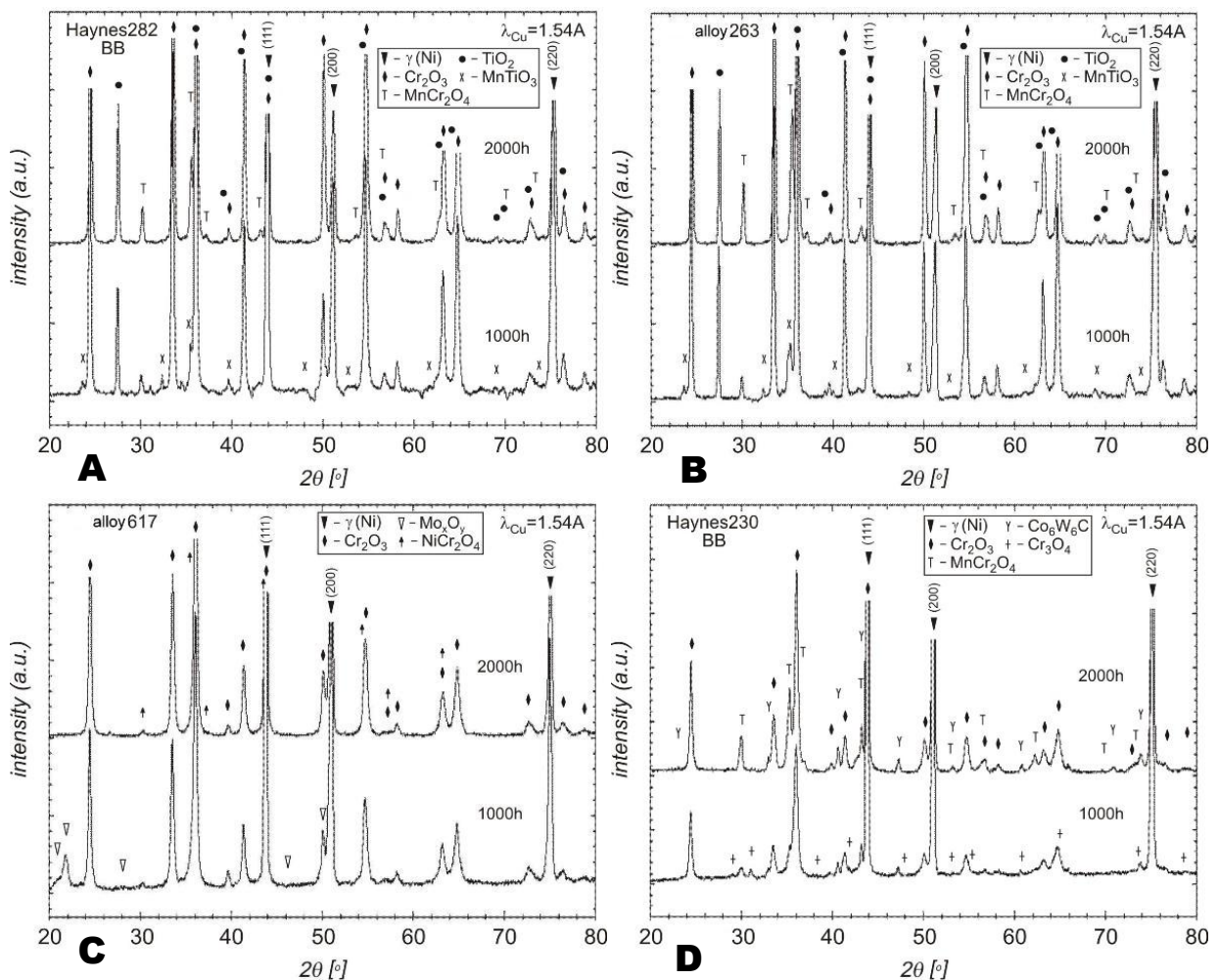


Figure 5 XRD pattern for A) Haynes[®] 282[®], B) alloy 263, C) alloy 617, and D) Haynes[®] 230[®] after 1000 and 2000 hours at 800 °C in pure water steam conditions

The XRD patterns for Ni based alloys are in good relation with the outcomes from the EDS measurements. The investigations, confirm that mainly Cr₂O₃ phase has developed supporting corrosion resistance of the exposed alloys in the long-term test. In addition, TiO₂ has been

observed as a second main phase in two (γ') gamma - prime strengthened alloys: alloy 263 and Haynes[®] 282[®]. In addition two solid strengthened alloys: alloy 617 and Haynes[®] 230[®] indicating the presence of NiCr₂O₄ spinel and MnCr₂O₄ spinel respectively. Finally, the formation of a thin oxide scale after 2000 hours test has been confirmed under XRD investigations due to observation of hard composite carbide η phase Co₆W₆C [10] deriving from the metal matrix.

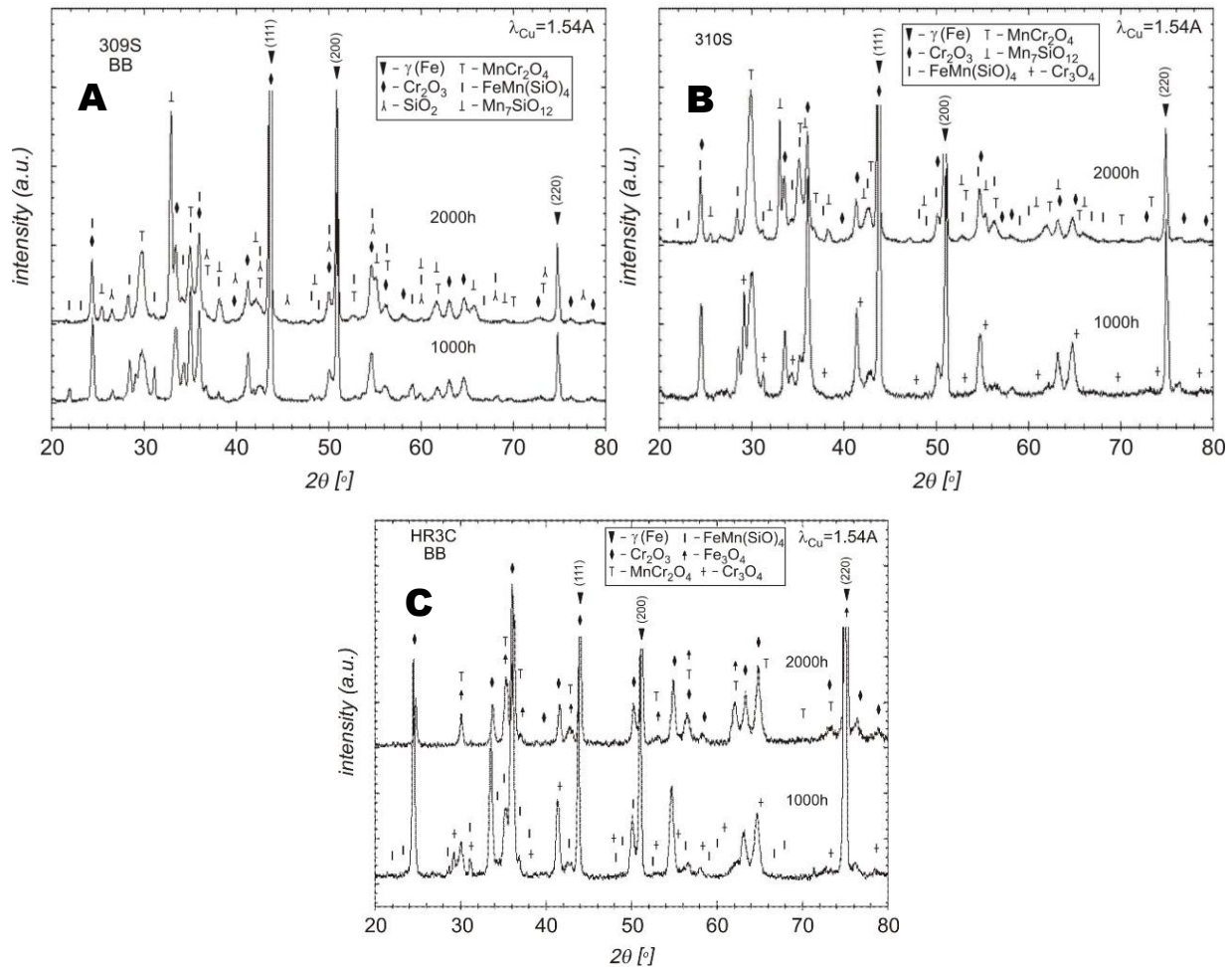


Figure 6 XRD patterns for A) 309S, B) 310S, C) HR3C exposed at 1000 and 2000 hours at 800 °C in pure water steam conditions

Furthermore, the results show that in Ni based alloys four phases have been observed mainly: Cr₂O₃, MnCr₂O₄, MnTiO₃ and TiO₂. The exposure of advanced steels under steam oxidation conditions developed mainly FeCr₂O₄, MnCr₂O₄ spinel phases and highly protective Cr₂O₃. The XRD investigation have been performed using Bragg Brentano theta-theta configuration in which the sample is stationary while the X-ray tube and the detector are rotated around it. Furthermore, the XRD investigation showed, that during the exposure some peaks are weaker after 2000 hours than that observed after 1000 hours exposure. In HR3C steel Cr₂O₃ peak is stronger after 1000 hours than that after 2000 hours, similar to γ (Fe) peak. In contrast, Cr₃O₄ is stronger after 1000 hours than after 2000 hours, such behaviour suggests that firstly formation of Cr₃O₄. In oxygen rich environment (water steam system) chromium develops wide range of oxide phase with different molar ratios Cr:O from 3:1 to 1:3. These oxides have different thermal stability. When phases consists high oxygen level Cr:O 2:3 such as CrO₃, Cr₈O₂₁, Cr₅O₁₂ and CrO₂) decompose almost completely at low temperatures, therefore,

formation of such oxide for high temperature application cannot be considered. Furthermore, such oxide may form during cooling the Fe-Cr rich alloys to room temperature. The stability of Cr-O oxides increases when Cr:O ratio increases, Cr_2O_3 is the most stable oxide, Cr_3O_4 is stable only at high temperature (2000 °C in narrow range of Cr:O ratio), at lower temperature during cooling Cr_3O_4 decomposes to Cr and Cr_2O_3 phase [11]. The considered Cr_3O_4 oxide might be described as CrCr_2O_4 or $\text{CrO}\cdot\text{Cr}_2\text{O}_3$. **Figure 7** shows Cr-O phase diagram found in FACTSAGE SGnucl-SGTE nuclear database 2004.

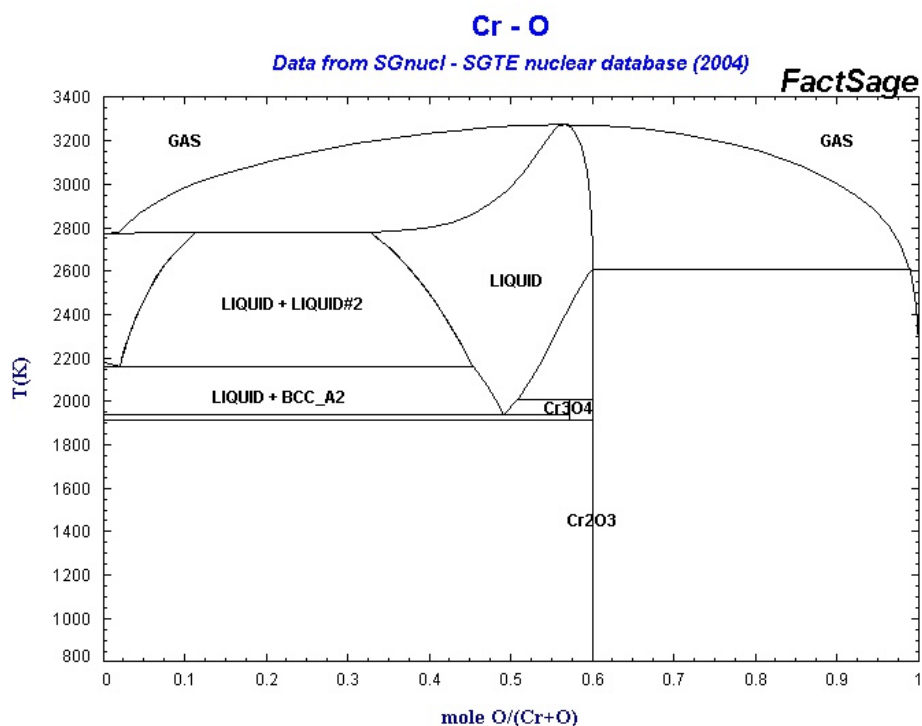


Figure 7 Cr-O phase diagram presenting Cr_2O_3 stability at 800 °C

The performed XRD analyses shown in **Figures 5 and 6** indicate that γ (Fe) as well as γ (Ni) phases have been observed, the both phases are weaker with exposure time from 1000 – 2000 hours. The observed results indicated that both Ni based and Fe based alloys construct relatively thin oxide scale transparent for by x-rays. Finally, minor phases such as $(\text{Mn,Fe})\text{SiO}_4$ or SiO_2 have been observed in trace quantities compared to Cr_2O_3 and spinel phases.

Cross-section analyses

Figures 8 and 9 show cross-section SEM images in BSE mode of the exposed Ni based and Fe based materials at 800 °C for 2000 hours respectively.

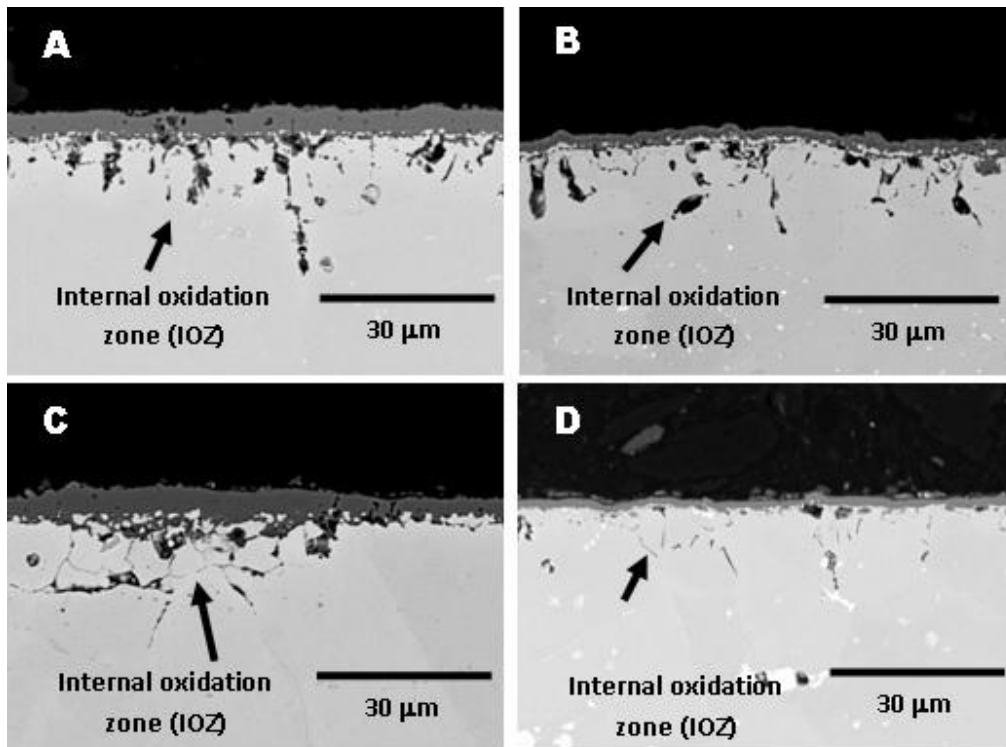


Figure 8 Cross-section microstructures developed at 800 °C for 2000 hours in steam atmosphere for: A) Haynes[®] 282[®], B) alloy 617, C) alloy 263, and D) Haynes[®] 230[®]

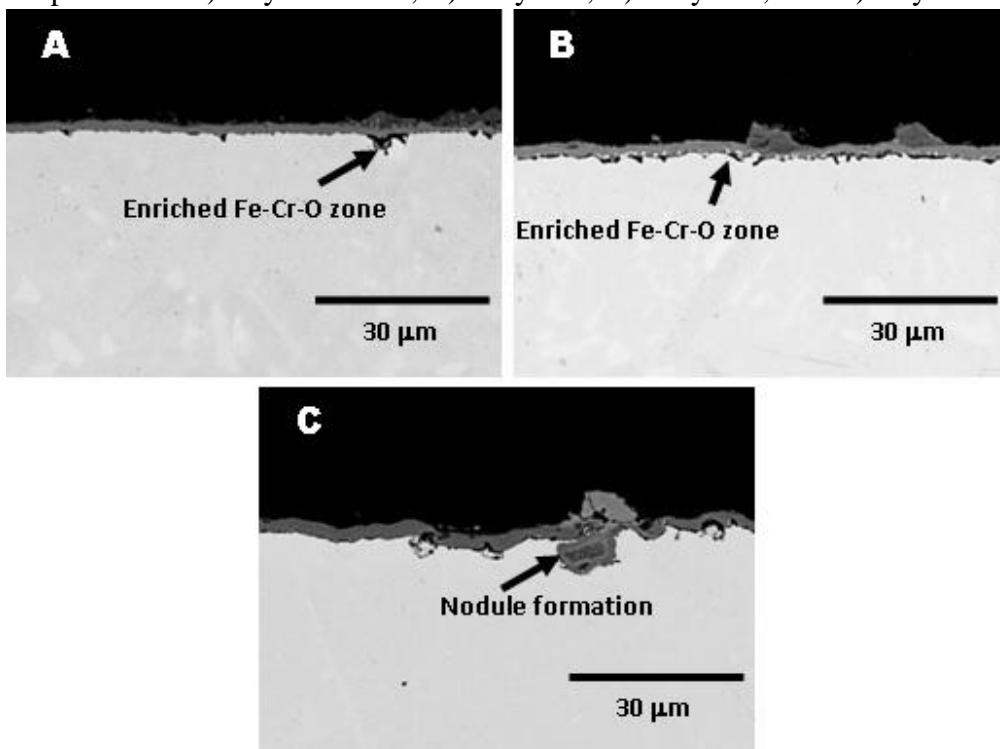


Figure 9 Cross-section microstructures developed at 800 °C for 2000 hours in steam atmosphere for: A) 309S, B) 310S and C) HR3C steel

The performed investigations on cross-sectioned materials revealed, that Ni based alloys underwent internal oxide penetration at 800 °C for 2000 hours. The highest degree of internal oxidation zone has been observed in the two (γ') gamma - prime strengthened alloys; alloy 263 and Haynes[®] 282[®], moreover in one solid-solution strengthened alloy in alloy 617 high degree of internal oxidation zone has been observed as well. During steam oxidation process at 800 °C, only solid-solution strengthened alloy Haynes[®] 230[®] showed some internal oxidation resistance. Internal oxidation process is unbeneficial for high temperature corrosion due to several aspects:

- May lead to thermal fatigue under severe thermal cycling conditions
- Decreases concentration of vital elements (Al, Cr), reduces possibility of adherent scale formation due to depletion of vital elements,
- Increases possibility of higher degree of corrosion in advanced materials rich in Cr and Al,
- Increases kinetics of advanced structural materials exposed at high temperatures.

Internal oxidation has been reported earlier [12]. Internal oxidation due to development, precipitation of oxides inside the material is always accompanied by changes in a volume of expansion. The volume of expansion generates stresses, which must be somehow released. Shida et al. [13, 14] suggested stress relief mechanisms of grain boundary sliding and extrusion of internal oxide-free metal adjacent to grain boundaries, in the case of intergranular oxidation. It has been observed, that mostly Al, Ti and Ni has been oxidised internally suggesting the formation of Al_2O_3 , TiO_2 and NiO phases. In contrast to Ni based alloys, advanced steels showed the formation of thinner oxide scales and lack of internal oxidation zone formation. The steels with high Cr content showed formation of thin oxide scale with thickness of 3 μm only. Some areas of the oxide scale have been covered by tiny nodules, suggesting enrichment of Fe in the oxide scale [15]. The formation of Fe rich oxide granules may inform about breakaway mechanism: the transition from protective oxidation, due to the exclusive formation of a Cr_2O_3 scale, to fast oxidation, characterised by the rapid growth of iron-rich oxides [16]. Nevertheless the number of nodules have been found to be relatively low as for the exposure duration, therefore the advanced steels exposed in this work showed better corrosion resistance than that offered by Ni based alloys in terms of corrosion resistance. The better corrosion resistance resulting in addition from the formation of dense, adherent scale consisting of the following phases: MnCr_2O_4 and Cr_2O_3 mainly, Fe-Cr-O region suggesting the formation of FeCr_2O_4 spinel zone that has been observed underneath the Cr_2O_3 rich oxide scale, the region consisted around 7 wt% Ni. In contrast, in Ni based alloys besides high degree of internal oxidation process development of highly defected, fast growing TiO_2 , MnTiO_3 have been observed. The formation of SiO_2 and other phases with Si (Fe,MnSiO_4) in advanced steel containing Si is reported in this study. Henry et al. [17] has shown that addition of Si to the metal matrix of 15 wt% Cr steels supporting breakaway oxidation resistance. In fact, addition of tiny Si quantities to 309S and 310S steels (> 20 wt% Cr) further enhanced the breakaway process, not only because of high Cr content and high activity and formation of stable Cr_2O_3 , but also due to the effect of Si. The exposed materials, shown lack of evaporation of Cr from the metal matrix or from Cr_2O_3 phase due to the formation of $\text{CrO}_2(\text{OH})_2$ (g) phase. Lack of evaporation process is probably due to the formation of MnCr_2O_4 spinel under steam oxidation conditions. The effect of Mn addition has been postulated earlier by Yang et al. [18]. It has been found that additions of Mn to the metal matrix of advanced Ni based alloys or advanced steels facilitated the formation of a bi-layered oxide scale, where an outer consisted M_3O_4 (M=Mn, Cr, Ni) spinel-rich layer at the oxide – gas interface over a Cr_2O_3 -rich sub-layer at the metal – oxide interface. Gordon et al. [19],

reported, that Mn additions to an alloy can reduce the activity of chromium in the oxide, due to the replacement of chromium with manganese from solid solution when low levels of manganese are added, or due to the formation of manganese-chromium spinel when high levels of manganese are added. Reduction in chromium activity leads to reduction in chromium evaporation by a factor of 35 at 800 °C. Similarly, the effect of FeCr₂O₄ spinel formation may reduce Cr activity and reduce evaporation from the oxide scale containing rich concentration of Cr, leading to enhancement of corrosion resistance. Finally, two (γ') gamma - prime strengthened alloys, have indicated the thickest oxide scale, the thickness of the exposed Ni based alloys exceeded doubled the thickness of the oxide scales developed on solid-solution strengthened Ni based alloys, the oxide scale has reached thickness higher than that observed in advanced steels. The results obtained in this work clearly indicate that the formation of MnCr₂O₄ spinel induces higher effect in mass gain reduction and supports higher corrosion resistance in steels type 309S, 310S than that observed in Ni based type; alloy 263 and Haynes[®] 282[®]. The formation of fast growing TiO₂ phase in two (γ') gamma - prime strengthened alloys privilege and obscure the beneficial effect observed via the formation of MnCr₂O₄ phase.

4. Conclusions

The aim of this paper was to show phase development under steam oxidation of Ni based alloys and high alloyed austenitic steels; where alloy 617 and Haynes[®] 230[®] are solid solution strengthened materials, while 263 and Haynes[®] 282[®] are precipitation strengthened alloys. Based on the results obtained after 2000 hours at 800 °C steam oxidation test the following conclusions can be made:

- All of the exposed high alloyed steels and Ni based alloys showed low mass gain at high temperature for 2000 hours,
- No spallation, delamination of cracks on the exposed surfaces or cross-sections have been observed
- No evaporation of Cr via the formation of CrO₂(OH)₂ (g) phase was observed,
- High alloyed steels showed the formation of protective scales where lack of spallation occurred, however some nodules formation has been potted
- Ni based alloys showed the following phases under XRD investigations:
 - Haynes[®] 230[®]: Cr₂O₃, and MnCr₂O₄, Co₆W₆C (trace quantities)
 - alloy 263: Cr₂O₃, MnTiO₃, MnCr₂O₄, TiO₂ and γ(Ni)
 - alloy 617: Cr₂O₃, NiCr₂O₄
 - Haynes[®] 282[®]: Cr₂O₃, MnTiO₃, MnCr₂O₄, and TiO₂
- Two (γ') gamma - prime strengthened alloys showed higher weight gain kinetics in contrast with two solid-solution strengthened alloys
- Stronger effect of TiO₂ phase formation in two (γ') gamma - prime strengthened alloys than MnCr₂O₄ effect has been observed
- No Co effect despite of high concentration of cobalt in alloy 263 and alloy 617 has been observed,
- No evaporation of Cr based phase from Fe and Ni based alloy probably due to the formation of MnCr₂O₄, FeCr₂O₄ spinel under steam oxidation conditions,
- Fe based materials showed the development of the following phases under XRD investigations:
 - 309S: Cr₂O₃, MnCr₂O₄, γ(Fe), SiO₂, Fe, Mn(SiO)₄ (trace quantities)
 - 310S: Cr₂O₃, MnCr₂O₄, γ(Fe), SiO₂ (trace quantities)
 - HR3C: Cr₂O₃, MnCr₂O₄, γ(Fe), Fe₃O₄, Fe₂O₃, Fe, Mn(SiO)₄ (trace quantities)

Acknowledgment

Authors like to acknowledge the support of fundamental research performed in this study to National Science Centre in Poland. Project number: 2014/13/D/ST8/03256. The author of the work acknowledges as well materials suppliers Haynes International USA, Sandmeyer Steel Company USA and Institute for Ferrous Metallurgy Poland.

Furthermore, the authors would like to acknowledge Prof. W. Ratuszek. Dr M. Witkowska, K. Chrusciel, from University Science and Technology for XRD analyses performed to this work

References

- [1] N. Komai, F. Masuyama, M. Igarashi, *Journal of Pressure Vessel Technology*, **127** (2005) 190.
- [2] J. Gabrel, C. Coussement, L. Verelst, R. Blum, Q. Chen, C. Testani, *Materials Science Forum*, **369-372** (2001) 931.
- [3] W. Quadackers, P. Ennis, J. Zurek, M. Michalik, *Materials at High Temperatures*, **22** (2005) 27-33.
- [4] I. Wright, A. Sabau, R. Dooley, *Materials Science Forum*, **595-598** (2008) 387-395.
- [5] I. G. Wright, P. J. Maziasz, F. V. Ellis, T. B. Gibbons, D. A. Woodford, 29th International Technical Conference on Coal Utilization and fuel systems (2004).
- [6] T. U. Kern, K. Weighthardt, H. Kirchner, *Proceedings of the 4th International Conference on Advances in Materials Technology for Fossil Power Plants*. Hilton Head Island, USA (2004)
- [7] I. Wright, R. Dooley, *Institute of Materials, Minerals and Mining and ASM International*, (2010)
- [8] H. Asteman, J. E. Svensson, L. G. Johansson, and M. Norell, *Oxidation of Metals*, **52(1/2)** (1999) 95
- [9] M. Lukaszewicz, N. J. Simms T. Dudziak, J. R. Nicholls, *Oxidation of Metals*, **79(5/6)** (2013) 473.
- [10] H. Yu, R. Ahmed, H. de Villiers Lovelock, S. Davies, *Journal of Tribology*, **131(1)** (2009) 1.
- [11] *Handbook of Ferroalloys, Theory and Technology*, 1st Edition, Edited M Gasik Elsevier, (2013)
- [12] D. J. Young, *High Temperature Oxidation and Corrosion of Metals*, Chapter 6 Alloy Oxidation II: Internal Oxidation, , Elsevier 2016
- [13] F.H. Stott, Y. Shida, D.P. Whittle, G.C. Wood, B.D. Bastow, *Oxidation of Metals*, **18(3/4)** (1982) 127.
- [14] Y. Shida, F.H. Stott, B.D. Bastow, D.P. Whittle and G.C. Wood, *Oxidation of Metals*, **18(3/4)** (1982) 93.
- [15] P. Tomaszewicz, G. R. Wailwork, *Oxidation of Metals*, **19(5/6)** (1983) 165.
- [16] T. Gheno, D. Monceau, D. J. Young, *Corrosion Science* **77** (2013) 246.
- [17] S. Henry, A. Galerie, L. Antoni, *Materials Science Forum* **369-372**, (2001) 353
- [18] Z.G. Yang, G.G. Xia, J.W. Stevenson, P. Singh, U.S. Department of Energy, PNNL-15304 (2005)
- [19] G. R. Holcomb, D. E. Alman, Department of Energy DOE/ARC-05-002